BioGecko

Vol 12 Issue 03 2023

ISSN NO: 2230-5807

APPLICATIONS OF ARTIFICIAL INTELLIGENCE TECHNIQUES TO EVALUATE MECHANICAL PROPERTIES OF ULTRA HIGH STRENGTH CONCRETE

G. Prabha[1], Dr.S. Thenmozhi[2], Sonal Banchhor[3], Akhil Maheshwari[4], Swapnil Balkrishna Gorade[5]
[1]Assistant Professor, Department of Civil Engineering,Easwari Engineering College, Bharathi Salai Ramapuram, Chennai, India-89,Email: prabhagandhi1985@gmail.com
[2]Associate Professor, Department of Civil Engineering, St.Joseph's College of Engineering, OMR, Chennai, India-600 119.
[3]Assistant Professor, Guru Ghasidas Vishwavidyalaya, Bilaspur, Chhattisgarh, India.
[4]Assistant Professor, Department of Civil Engineering, Sangam University, Bhilwara, Rajasthan,India.
[5]Assistant Professor, Pimpri Chinchwad College of Engineering,Sector no-26,NigdiPradhikaran, Pune,Maharashtra, India-411044, Email:sbgorade7@gmail.com

Abstract: Predicting the flexural strength and compressive strength of ultra-high performance steel fiber reinforced concrete (UHPFRC) accurately has a significant impact on controlling steel fiber volume fraction and optimizing UHPFRC mix proportion. Steel fibers increase the flexural strength, compressive strength, and ductility of ultra-high-performance concrete. Two artificial neural networks were created in this study to forecast the flexural strength and compressive strength of UHPFRC, respectively, in order to assess the impacts of steel fibers on the mechanical characteristics of UHPFRC. The flexural strength model and the compressive strength model were developed using 102 test data sets and 162 test data sets from the literature, respectively. The compressive strength and flexural strength of UHPFRC were the results of these two models, which looked at the influential parameters such as the water to binder ratio, the diameter, the length, the aspect ratio, and the volume fraction of steel fibres as well as the compressive and flexural strengths of concrete without fibres as inputs. The findings demonstrate that the artificial neural network models correctly anticipated UHPFRC's compressive and flexural strengths. The suggested models were found to have good application and reliability with regard to forecasting the compressive strength and the flexural strength of UHPFRC by comparison with current analytical models.

Keywords: artificial neural model; compressive strength; flexural strength; ultra-high-performance concrete; steel fiber

1 INTRODUCTION

Compressive strength and flexural strength are two essential mechanic criteria to assess the strength and ductility of materials in ultra-high-performance concrete (UHPC) mixture design. UHPC is brittle, thus to make it more ductile and stronger, steel fibres with high tensile strength and ultimate elongation are always uniformly scattered in UHPC. Ultra-high performance steel fibre reinforced concrete, or UHPFRC, is another name for UHPC reinforced with steel fibres. The steel fibres in UHPFRC modify the granular skeleton, enhance the cohesive forces between the fibres and the matrix, and lengthen the anchoring between the fibres and the surrounding matrix [1,2]. Additionally, steel fibres act as a crack filler and slow the spread of cracks to improve the ductility and strength of UHPFRC [3]. Unfortunately, using too many steel fibres causes the fibres to interlock and interwrap, reducing the workability of UHPFRC and weakening it [4]. Additionally, the expense of adding a lot of steel fibres to the UHPFRC is too high since they are costly. In order to regulate the volume fraction of steel fibres, optimise mix proportion, and lower UHPFRC costs, it is necessary to precisely anticipate the compressive strength and flexural strength of UHPFRC. However, because to the complicated composite behaviour brought on by the parameters of steel

fibres (diameter (D), length (L), aspect ratio (AR), etc.), assessing the flexural strength and compressive strength of the UHPFRC is a significant difficulty.

The sustainability contribution of cement-based materials is a current research area [5-8] and it has been determined that a number of additions to cement-based materials, such as silica fume, fly ash, the water to cement ratio, and others, perform well enough to be used in high performance concrete. Due to this aspect, it is also important to take into account their impact on the mechanical characteristics of these novel concretes. The compressive strength and flexural strength of UHPFRC have been the subject of several experimental and theoretical studies over the past few decades [9–30]. The compressive strength and flexural strength of UHPFRC have been predicted using a number of analytical models that have been developed by making a number of assumptions about the process and creating equilibrium equations. Additionally, based on the experimental research, a number of empirical models [31-36], some of which are included in the design codes, have been developed to forecast the compressive strength and the flexural strength of UHPFRC. Furthermore, the JGJ/T 221 [31] Chinese standard only suggests an empirical methodology to forecast the flexural strength of steel fibre reinforced concrete. These models often rely heavily on the diameter, length, volume percentage, and compressive/flexural strength of UHPFRC without fibres. The experimental data utilised to develop the empirical formula, however, is sparse, with the majority of them concentrating solely on the volume percent of steel fibres and ignoring other factors. Thus, the prediction accuracy and dependability of such empirical models are evaluated when new test data are available.

The goal of this project is to create two ANN models to forecast UHPFRC's compressive and flexural strengths. The development of models and evaluation of the impacts of steel fibres on the compressive strength and flexural strength of UHPFRC, respectively, required the collection of 162 compressive strength data sets and 102 flexural strength data sets from published literature. To assess the suggested models' dependability and predictability, they were compared to a number of analytical models. Additionally, the ANN models may be used to optimise the UHPFRC mixes, identify the volume percent of steel fibres in UHPFRC, and forecast the flexural strength and compressive strength of UHPC.

2. Artificial Neural Network Approach

A machine learning technique known as an artificial neural network (ANN) was developed in an effort to replicate the nervous system of a person in order to interpret experimental data by classifying, grouping, regressing, and forecasting [43]. One common ANN is the multi-layer feed-forward perception network, which comprises an input layer, one or more hidden layers, and an output layer. The many neurons are dispersed across the layers of this network (see Figure 1). There is no connection between neurons in the same layer of the network; instead, all neurons in each layer are linked to the one below. By altering the weights and thresholds between layers, the input layer and the output layer are converted. A set of weights will be steady and a positive outcome will be attained if the issue can be learned.

The back propagation neural network, which employs nonlinear training techniques, is one of the most fundamental and crucial neural networks for multi-layer feed-forward networks. The back propagation network's training procedure is based on supervised learning, which reduces errors between estimated and experimental values by periodically modifying the weights by a modest amount [40,41].

A back propagation network's training procedures are divided into two stages: the forward stage and the backward stage. The forward stage uses the supplied starting connection weights and the input data to calculate the network outputs. The input data is transferred during the procedure from the input layer to the concealed layer. The neurons in the hidden layer then add up the input data in a weighted total, apply an activation function to the sum, and then send the results of the activation to the output layer. Equation (1) may be used to determine the input data's weighted sum [43–46].

$$netj = \sum \omega ijxi + bj \quad (1)$$

where xi is the output of the ith neuron in the lower layer, bj is the bias of the jth layer in the upper layer, netj is the weighted sum of the jth neuron received from the lower layer with n neurons, ij is

the weight between the ith neuron in the lower layer and the jth neuron in the upper layer. Sigmoid or linear functions are frequently used as the activation function in back propagation networks. Equation (2) may be used to represent the Sigmoid function.

$$netj = \sum \omega ijxi + bj \quad (2)$$

$$oj = \frac{1}{1 + e^{-netj}} \quad (3)$$

where $o_j$is the output of the j_{th}neuron in the upper layer.

estimated errors between estimated outputs and experimental findings are transmitted back to the network in the backward step to change connection weights and bias. Until the mistakes are at a level that is acceptable, this procedure is repeated. Equation (4) can be used to summarise the weights' adjusted value.

$$\Delta\omega_{ij}(n) = \eta \times \delta_J^j \times o^i{}_I \quad (4)$$

where $\Delta\omega_{ij}$is the n_{th} value of weights adjustment between the i_{th}neuron in the lower layer and the j_{th} j ^{i}is the neuron in the upper layer, η is the training rate, $\delta_J$is the local gradient of the j_{th}layer, and $o_I$output of the input neurons.

Because the LM algorithm combines the benefits of the Quasi-Newton algorithm with the Steepest Descent Back-propagation, which is suited for non-linear least square problems and curve fitting, it is used in this work as the training approach for the ANN models.

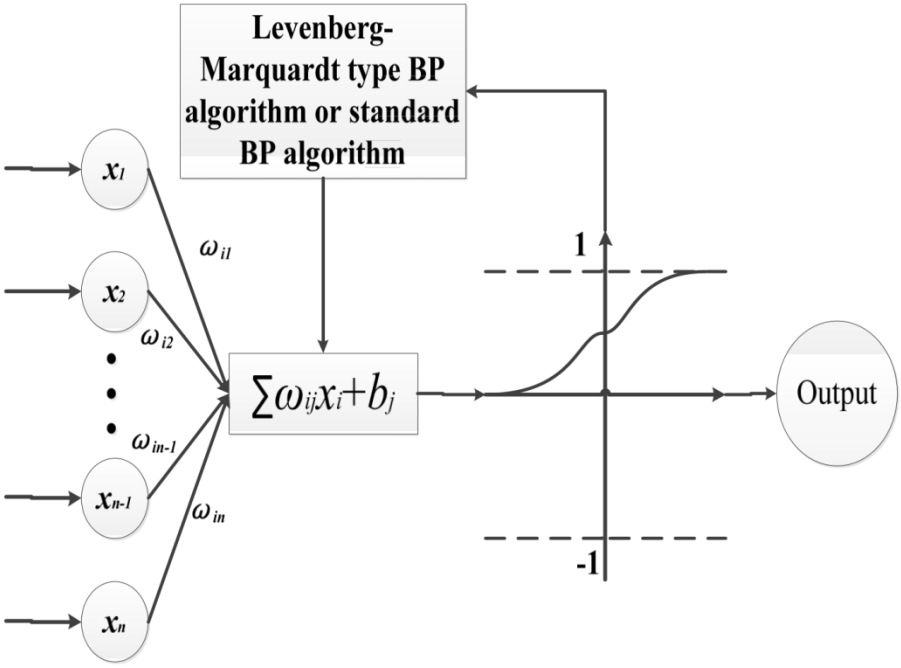

Figure 1. System of typical artificial neural networks (ANN) model. A typical ANN model has input, sum function, log-sigmoid activation function, and output.

3. Database and Models

3.1. Data Collection

A trustworthy database was created in order to investigate how steel fibres affect the compressive strength and flexural strength of UHPFRC. The literature [9–30] was searched for 162 group compressive strength experimental data and 102 group flexural strength experimental data (Tables 1 and 2).

Due to a lack of appropriate standards, the specimens used for compressive strength testing come in a variety of sizes and forms. In accordance with GB/T 31387 [47], a cube specimen of 100 x 100 x 100 mm is regarded as the industry standard for data homogeneity. By using the correlation

approaches recommended by researchers [48–51], the test specimens were converted to standard cube compressive strength, and the resulting equations are as follows.

$$fcu,100 = 0.959fcu,70.7 \quad (5)$$

$$f_c^0 = 0.845f_{cu},70.7 \quad (6)$$

$$fcu,150 = 0.91fcu,100 + 3.62 \quad (7)$$

$$fcu,150 = fcylin,100\times200 + 6.41 \quad (8)$$

$$fcylin,50\times100 = 1.07fcylin,100\times200 \quad (9)$$

where, $f_{cu,70.7}$ $f_{cu,100}$, and $f_{cu,150}$ are the compressive strength of 70.7 mm cube, 100 mm cube, and 150 mm cube, respectively; fc0 is the axis compressive strength of UHPFRC; the size effects are not readily apparent in fc0. fcylin,50100 and fcylin,100200 are the compressive strengths of 50 100 mm and 100 200 mm cylinder, respectively.

To create the training-testing database, a total of 166 experimental compressive strength data sets and 102 experimental flexural strength data sets were acquired. The remaining data sets (20% of the total data) were utilised for testing, while 80% of the data (133 and 80) were chosen as training sets. To counteract the impact of arbitrary selection on the outcomes, the testing data were chosen at random. According to pre-existing calculation models [31–38], the water to binder ratio (W/B), the diameter, length, aspect ratio, and volume fraction of steel fibres, as well as the compressive strength (PCS) or flexural strength (PFS) of UHPFRC without steel fibres, were chosen as the main input parameters, and the compressive strength (CS) or flexural strength (FS) of UHPFRC was used as the output variable. The ranges of the input and output variables in the databases for compressive strength and flexural strength used in this investigation are displayed in Table 3.

Table 1. Ranges of Parameters in Compressive Strength and Flexural Strength Data base.

Variables	Compressive Strength		Flexural Strength	
	Minimum	Maximum	Minimum	Maximum
W/*B*	0.13	0.30	—	—
D/mm	0.15	0.65	0.16	0.65
L/mm	6	30	9	30
AR	100	30	32.5	100
VF/%	0.00	5.00	0.00	5.00
PCS/MPa	72.15	220.98	8.23	26.88
CS/MPa	72.15	249.68	8.23	73.67

3.2. Proposed ANN Model

Three layers make up the ANN models suggested in this paper: an input layer, a hidden layer, and an output layer (see Figure 1). The specifications of the research questions define the number of input and output nodes. The initial number of hidden layer nodes should be determined through experiments, though, as there aren't any solid mathematical procedures for computing this amount. In the hidden layer, the linear activation function is utilised, and in the output layer, the log-sigmoid activation function.

A series of tests were conducted to establish the number of layers and other parameters of the ANN models by the least mean square error (MSE) of the training data in order to construct the ANN model for forecasting the flexural strength and compressive strength of UHPFRC. The flexural strength (FS) of UHPFRC is investigated as an output, while the length (L), diameter (D), aspect ratio (AR), volume fraction (VF), and steel fibre volume fraction are investigated as inputs. Additionally, the water to binder ratio (W/B) and compressive strength (PCS) of UHPFRC without fibres are investigated. The characteristics of the ANN models used to forecast the compressive and flexural strengths of UHPFRC are provided in Table 4 along with the models' structures in Figure 2.

Table 2. Parameters used in the ANN models.

Parameters	Flexural Strength Model	Compressive Strength Model
Number of input layer nodes	5	6
Number of hidden layers	1	1
Number of hidden layer nodes	15	20
Number of output layer nodes	1	1
Momentum factor	0.8	0.6
Learning rate	0.3	0.3
Target error	0.00001	0.00001
Learning cycle	10,000	10,000

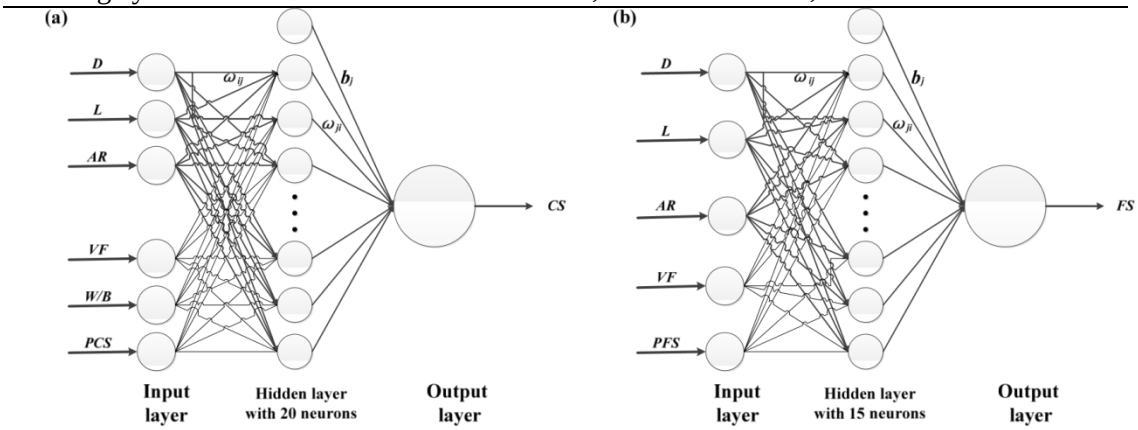

Figure 2. Structure of ANN models, (**a**) Compressive strength ANN model, (**b**) Flexural strength

ANN model; W/B (water to binder ratio); PCS (compressive strength of UHPFRC without fibers);

VF (volume fractions); AR (aspect ratio); PFS (flexural strength of UHPFRC without fibers); CS

(Compressive strength of UHPFRC); FS (flexural strength of UHPFRC). In (**a**), the compressive strength ANN model developed in this study has three layers with six neurons in input layer, twenty neurons in hidden layer and one neural in output layer; in (**b**), the compressive strength ANN model that was developed in this study has three layers with five neurons in input layer, fifteen neurons in hidden layer, and one neural in output layer. In these two figures, $\omega_{ij}$is the weight between the i_{th}neuron in the input layer and the j_{th}neuron in the hidden layer, $\omega_{ji}$is the weight between the i_{th}neuron in the hidden layer and the j_{th}neuron in the output layer, and $b_j$is the bias of the j_{th}layer in the output layer.

3.3. Processing Data

The gathered data used to create ANN models should be normalised within the predetermined bounds to remove non-singular data, increase the accuracy of findings, speed up convergence, and shorten computation times. Linear or logarithmic functions make up the majority ofnormalisation expressions [43]. In this study, the data were normalised using a sample function, as shown in Equation (10).

$$X_i,norm = 0.1 + 0.8 \times (X_i - X_{min})/(X_{max} - X_{min}) \quad (10)$$

where $X_{i,norm}$is normalized data and $X_{max}$and $X_{min}$are the maximum and minimum value of data, respectively. An inverse normalized process is applied to the output layer to get the test data.

4. Results and Discussion

4.1. Results Assessment Criteria

In addition to the input data used in the training process, a correctly trained ANN model should provide an accurate output prediction for fresh testing data outside the training database. In this work, five indicators were used to assess the performance of the flexural strength ANN model and

six indications were used to assess the performance of the compressive strength ANN model. These three metrics, which are determined by Equations (11) through (13), are the root mean square error (RMS), absolute fraction of variance (R2), and integral absolute error (IAE), respectively [38,45]. The suggested models are said to properly predict the experimental data when the RMS and IAE tend to zero and the R2 tends to one.

4.2. Results Evaluation

4.2.1. Predicting Model for Compressive Strength

The compressive strength ANN model created in this work was used to assess how steel fibres affected UHPFRC's compressive strength. Figure 3 displays comparisons between the experimental and predicted values for the training and test sets of the compressive strength ANN model. It was clear that the ANN model's projected values from the training and testing data were rather close to the goal values. By virtue of this phenomena, it was shown that the ANN model was capable of understanding the nonlinear relationship between the input and output variables. As a result, the ANN model had the capacity to predict how steel fibres would affect UHPFRC's compressive strength.

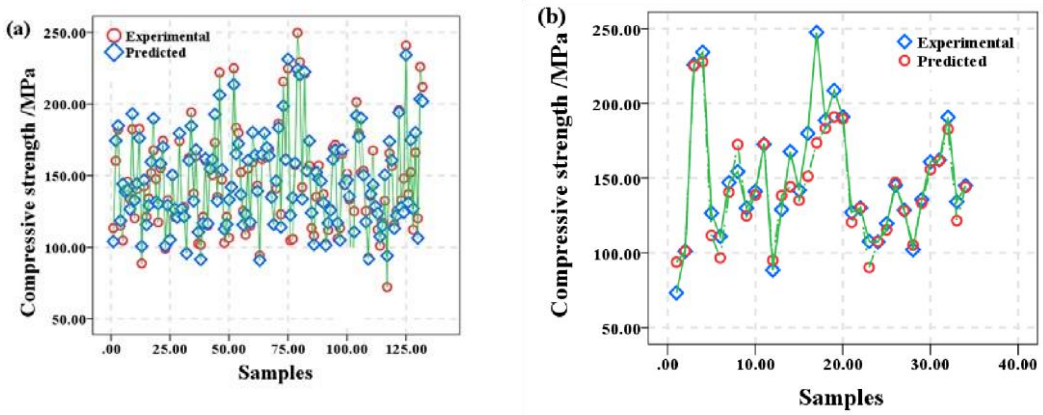

Figure 3. Comparison of predicted values from compressive strength ANN model with experimental results: (**a**) Training data, (**b**) Testing data. The figures show that the comparison between the target values and predicted values of testing and training data from experiments and compressive strength ANN model, the horizontal axis denotes number of training or testing data, and the vertical axis denotes the compressive strength. It was obvious that the predicted values accord with the target values.

Table 3. The indicators of training and testing of Compressive strength ANN model.

Indicators	Training	Testing
RMS	0.0876	0.0980
R2	0.9923	0.9901
IAE	0.0005	0.0019

4.2.2. Prediction Model for Flexural Strength

The flexural resistance The ANN model used in this work was used to forecast the UHPFRC's flexural strength. Figure 4 displays comparisons between the anticipated and experimental values for the ANN model's training and testing data. It was clear that the ANN model's projected values from the training and testing data were rather close to the desired values. By virtue of this phenomena, it was shown that the ANN model was capable of understanding the nonlinear relationship between the input and output variables. As a result, the ANN model had the capacity to predict how steel fibres would affect UHPFRC's flexural strength.

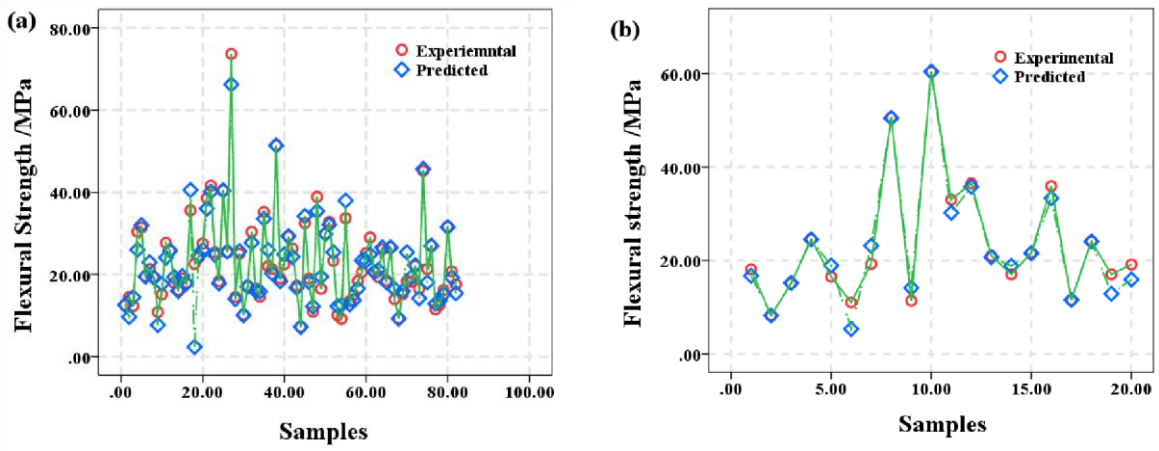

Figure 4. Comparison of predicted values from flexural strength ANN model with experimental results: (**a**) Training data, (**b**) Testing data. The figures showed that the comparison between the target values and predicted values of testing and training data from experiments and flexural strength ANN model, the horizontal axis denotes number of training or testing data and the vertical axis denotes the flexural strength. It was obvious that the predicted values accord with the target values.

RMS, R2, and IAE were presented in Table as the flexural strength ANN model's performance metrics for training and testing data. The metrics in Table 4 demonstrate that the suggested methodology delivered positive outcomes. As a result, the flexural strength of the ANN model examined in this work had excellent accuracy and was appropriate for assessing how steel fibres affected UHPFRC's flexural strength.

Table 4. The indicators of Training and Testing of Flexural strength ANN model.

Indicators	Training	Testing
RMS	0.1492	0.0376
R2	0.9777	0.9986
IAE	0.0011	0.0004

4.3. Comparison with Other Models

4.3.1. Compressive Strength Models

The findings from the compressive strength ANN model were compared with the values that were estimated by current models and given in the literature to evaluate the dependability of the suggested model [34–36]. The models for forecasting the compressive strength of steel fibre reinforced concrete (SFRC) are compiled in Table 7 since there are few models for predicting the compressive strength of UHPFRC. These models use the Nataraja model to predict the compressive strength (30–50 MPa) of SFRC, the Ezeldin model to predict the compressive strength (35–85 MPa), the VF ranges from 30 kg/m3 to 60 kg/m3, and the AR are 60, 75, and 100; Yuchen Qu model is applied to predict the compressive strength (30–50 MPa) of SFRC, the VF ranges from 0 to 3.4%, and the AR are from 50 to 100.

Table 5. Analytical models for predicting the compressive strength of steel fiber reinforced concrete (SFRC).

Analytical Model	Compressive Strength
Nataraja [34]	$f_{cf} = fc + 2.1604(RIw)$
Ezeldin [35]	$f_{cf} = fc + 3.51(RIw)$
Yuchen Qu [36]	$f_{cf} = fc + 2.35(RIv)$

Where f_{cf} and f_c are the compressive strength of SFRC and plain concrete, respectively; RI_w and RI_v are the reinforcing indexes of steel fibers weight fraction and steel fibers volume fraction,

respectively, $RI_w$is around 3.25 times of RI_v, $RI_w = w_f \times l_f/d_f$,$w_f$is the weight fraction of steel fibers, $l_f$is the length of steel fibers, and the $d_f$is the diameter of steel fibers.

Based on the data gathered, the analytical methods previously stated were used to determine the compressive strength of UHPFRC. The compressive strength ANN model from this work and the analytical models from prior studies are shown in Table 8 along with their respective means, standard deviations (SD), and IAE. In Table 9, the SD and the IAE were within the ranges of 0.1191-0.1268 and 1.03-1.34%, respectively, while the mean values for the analytical models ranged from 0.8830 to 0.9454, being less than one. The SD and IAE were relatively low, and the mean values from the ANN model in this investigation were quite near to one. Figure 5 shows that the anticipated values derived from the analytical models of earlier studies may undervalue the very variable experimental outcomes. The Nataraja model, Ezeldin model, and Yuchen Qu model all produced ranges of anticipated outcomes compared to experimental data that were 45-15%, 40-30%, and 50-10%, respectively. While the ANN model's range of projected outcomes in comparison to experimental findings is between 15 and 15%. The ANN model presented in this work could predict the behaviours of UHPFRC extremely well when compared to analytical methods for predicting the compressive strength of UHPFRC. As a result, the compressive strength ANN model's predictions have a high degree of accuracy and stability when used to assess how steel fibres affect the compressive strength of UHPFRC.

Table 6. The Mean value, standard deviation (SD), and integral absolute error (IAE) of ANN model and analytical models.

Models	*Mean*	*SD*	*IAE*
ANN model	1.0050	0.0896	0.70%
Nataraja model	0.9152	0.1191	1.13%
Ezeldin model	0.9454	0.1216	1.03%
Yuchen Qu model	0.8830	0.1268	1.34%

Table 9. Analytical models for predicting the Flexural strength of SFRC.

Analytical Model	Flexural Strength
JGJ/T 221 [31]	$f_{ff} = f_f(1 + 1.25V_f l_f/d_f)$
Swamy [32]	$f_{ff} = 0.97f_f(1 - V_f) + 3.41V_f l_f/d_f$
Won-Kya Chai [33]	$f_{ff} = f_f + 0.103V_f l_f/d_f$

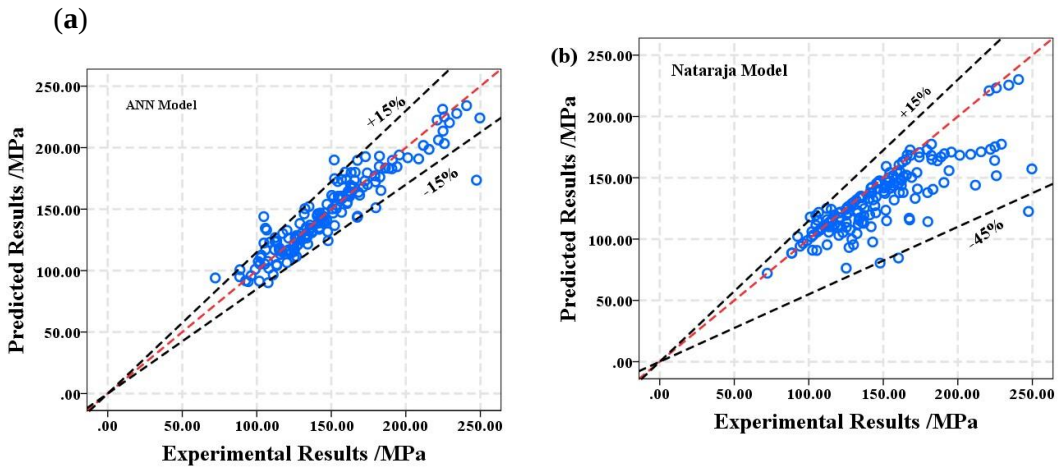

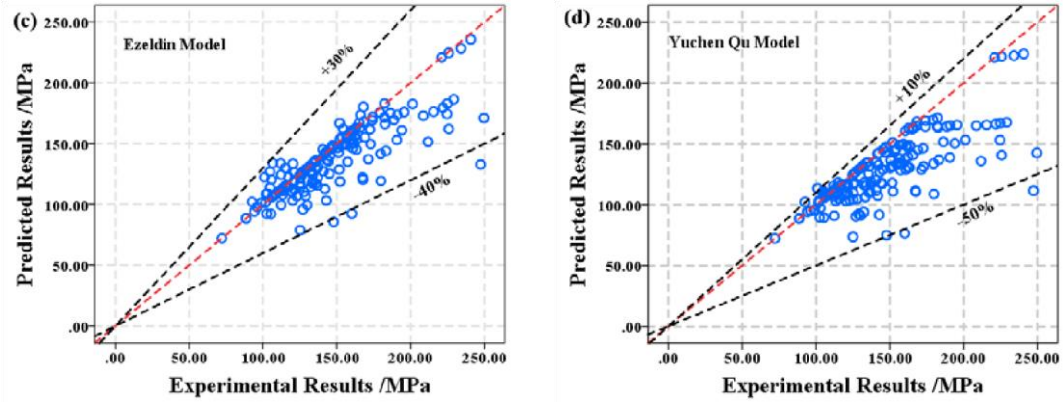

Figure 5. Comparison between predicted values and experimental values from three analytical models (proposed by Nataraja, Ezeldin, and Yuchen Qu) in previous studies and the ANN model studied in this paper. The 45 degree diagonal line (red line) denotes the predicted values equal to the experimental values and the black lines denote that the maximum ranges between predicted results and experimental results.

4.3.2. Flexural Strength Models

The findings from the flexural strength ANN model were compared with the values that were computed by current models given in the literature [31–33] in order to investigate the validity of the proposed model. The models for forecasting the flexural strength of steel fibre reinforced concrete (SFRC) are compiled in Table 9 as there are few models for predicting the flexural strength of UHPFRC.

Where $f_{f\,f}$ and f_f are the flexural strength of steel fiber reinforced concrete and plain concrete, respectively; V_f is the volume fraction of steel fibers, l_f is the length of steel fibers, and the d_f is the diameter of steel fibers.

Based on the data gathered, the analytical models previously stated were used to determine the flexural strength of UHPFRC. For the analytical models of earlier research and the flexural strength ANN model used in this investigation, Table 10 shows the mean value, standard deviation (SD), and IAE of fpredicted/fexperimental. In Table 10, the SD and IAE were within the ranges of 0.2055-0.4431 and 3.03-4.04%, respectively, while the mean values for the analytical models varied from 0.8429 to 1.1458. The SD and IAE were relatively low, and the mean values from the ANN model in this investigation were pretty near to one. Figure 6 shows that the anticipated values derived from the analytical models of earlier studies may significantly underestimate the very variable experimental outcomes. The JGJ/T 221 model, Swamy model, and Won-Kya Chai model have prediction ranges of 35-180%, 50-30%, and 35-150%, respectively, based on experimental data. While the ANN model's range of projected outcomes in comparison to experimental findings is between 15 and 15%. The ANN model suggested in this work could predict the flexural behaviour of UHPFRC extremely well when compared to the analytical models of flexural strength for UHPFRC. In order to assess the impacts of steel fibres on the flexural strength of UHPFRC, the predictions of the flexural strength ANN model are therefore very accurate and stable.

Table 10. The Mean value, SD, and IAE of ANN model and analytical models.

Models	*Mean*	*SD*	*IAE*
ANN model	0.9915	0.1509	1.50%
JGJ/T 221 model	1.2807	0.4431	4.04%
Swamy model	0.8429	0.2055	3.03%
Won-Kya Chai model	1.1458	0.3547	3.30%

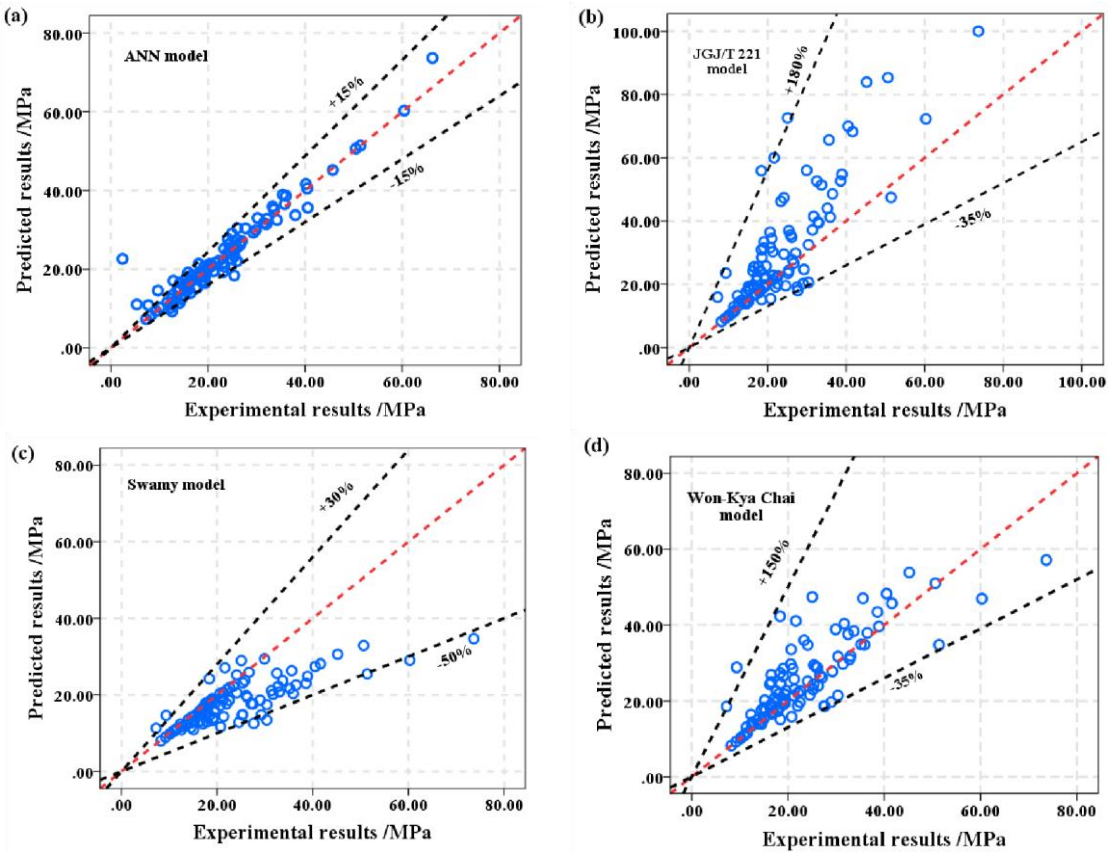

Figure 6. Comparison between predicted values and experimental values from three analytical models (proposed by JGJ/T 221, Swamy, Won-Kya Chai) in previous studies and the ANN model studied in this paper. The 45-degree diagonal line (red line) denotes the predicted values equal to the experimental values and the black lines denote that the maximum ranges between predicted results and experimental results.

5. Conclusions

In this study, the compressive and flexural strengths of UHPFRC were assessed using the ANN approach. 166 compressive strength data sets and 102 flexural strength data sets from prior research were used to create two reliable databases. Out of these, 133 and 80 samples were randomly selected for training and the remaining samples were used for testing to create the compressive strength ANN model and the flexural strength ANN model, respectively. Following were the conclusions:

(1) The compressive strength ANN model was trained by using the LM algorithm, with twenty neurons in hidden layers, revealing great prediction performance. The predicted values were fairly close to the experimental results for both the training and testing data sets in the proposed model.

(2) The flexural strength ANN model was trained by using the LM algorithm, with twenty neurons in hidden layers, revealing great prediction performance. The predicted values were fairly close to the experimental results for both the training and testing data sets in the proposed model.

(3) Three analytical models suggested in prior works were compared with the outcomes of the compressive strength ANN model. The comparison showed that, in contrast to the projected values from the ANN model in this work, which accord with the experimental values, the analytical models suggested by others may understate the compressive strength by around 10% on average.

(4) Three analytical models that were suggested in prior research were compared to the outcomes of the flexural strength ANN model. The comparison showed that, whereas the average values

of the analytical models put out by others may range from 0.8429 to 1.1458, those in this study's ANN model accord with the experimental results.

(5) The ANN models put out in this work offer a wide range of applicability and dependability when it comes to assessing how steel fibres affect the compressive strength and flexural strength of UHPFRC.

References

1. Zdeb, T. An analysis of the steam curing and autoclaving process parameters for reactive powder concretes. *Construct. Build. Mater.* **2017**, *131*, 758–766. [CrossRef]
2. Grünewald, S. *Performance-Based Design of Self-Compacting Fiber Reinforced Concrete*; Delft University of Technology: Delft, The Netherlands, 2004.
3. Yu, R.; Spiesz, P.; Brouwers, H.J.H. Mix design and properties assessment of Ultra-High Performance Fiber Reinforced Concrete. *Cem. Concr. Res.* **2014**, *56*, 29–39. [CrossRef]
4. Zhao, L.P.; Gao, D.Y.; Zhu, H.T. Effects of steel fibers on the strength and the ductility of concrete. *J. North Chin. Inst. Water Conserv. Hydroelectr. Power* **2012**, *33*, 29–32.
5. Ortega, J.M.; Sánchez, I.; Climent, M.A. Impedance spectroscopy study of the effect of environmental conditions in the microstructure development of OPC and slag cement mortars. *Materials* **2017**, *10*, 569–583. [CrossRef]
6. Sánchez, I. Influence of environment on durability of fly ash cement mortars. *ACI Mater. J.* **2012**, *109*, 647–656.
7. Joshaghani, A.; Balapour, M.; Ramezanianpour, A.A. Effects of controlled environmental conditions on mechanical, microstructural and durability properties of cement mortar. *Construct. Build. Mater.* **2018**, *164*, 134–149. [CrossRef]
8. Ramezanianpour, A.A.; Malhotra, V.M. Effects of curing on the compressive strength resistance to chloride-ion penetration and porosity of concrete incorporating slag, fly ash or silica fume. *Cem. Concr. Compos.* **1995**, *17*, 125–133. [CrossRef]
9. Bae, B.; Choi, H.K.; Choi, C.S. Correlation between tensile strength and compressive strength of ultra-high strength concrete reinforced with steel fiber. *J. Korea Concr. Inst.* **2015**, *27*, 253–263. [CrossRef]
10. Prem, P.R.; Bharatkumar, B.H.; Murthy, A.R. Influence of curing regime and steel fibers on the mechanical properties of UHPC. *Mag. Concr. Res.* **2015**, *67*, 988–1002. [CrossRef]
11. Ayira, O.J.F. Investigating the properties of reactive powder concrete (RPC) compressive and flexural strength.
Diss. Bachelor Eng. **2013**, *4*, 9758–9762.
12. Khalil, W.; Damha, L.S. Mechanical properties of reactive powder concrete with various steel fiber and silica fume contents. *ACTA TecniaCorviniensis Bull. Eng.* **2014**, *7*, 47–58.
13. Guo, J. Influence of compressive strength of reactive powder concrete with different fibers. *Concrete* **2016**, *5*, 87–90.
14. Ma, K.; Que, A.; Liu, C. Impact analysis of fibers on mechanical properties of reactive powder concrete.
Concrete **2016**, *3*, 76–83.
15. Zhong, S.; Wang, Y.; Gao, H. Effect of fibers on strength of self-compacting reactive powder concrete. *J. Build.*
Mater. **2008**, *11*, 522–527.
16. Wang, Q.; Guo, Z.; Xiang, Z.; Shao, J. Experimental research on proportion of reactive powder concrete 200 (RPC200). *J. Arch. Civil Eng. Depart.* **2007**, *1*, 70–74.
17. Huang, L.; Xing, F.; Deng, L.; Huang, P. Study on factors affecting the strength of reactive powder concrete. *J. Shenzhen Univ. Sci. Eng.* **2004**, *21*, 178–182.
18. Bi, Q.; Yang, Z.; Jiao, Q.; Wang, H. Experiment study on mechanical properties of a hubrid fiber reinforced reactive powder concrete. *J. DaLianJiaotong Univ.* **2009**, *30*, 19–21.
19. Zhang, P.; Kang, Q.; Shen, Z.; Wang, Z. Experimental research on the mechanical properties of steel fiber and carbon fiber reinforce RPC. *Funct. Mater.* **2010**, 233–235.

20. Wang, X.; Wang, Y. Mechanical properties of RPC with different steel fiber volume contents. *J. Build. Mater.* **2015**, *18*, 941–945.
21. Wang, J.; Hao, X.; Ji, F. Effects of steel fibers on the mechanical properties of reactive powder concrete.
Low Temp. Arch. Technol. **2018**, *3*, 18–20.
22. Jia, F.; AN, M.; Zhang, H.; Yu, Z. Effect of fibers on bond properties between steel bar and reactive powder concrete. *J. Build. Mater.* **2012**, *15*, 847–851.
23. Zhang, Q.; Wei, Y.; Zhang, J.; Feng, P. Influence of steel fiber content on fracture properties of RPC. *J. Build.*
Mater. **2014**, *17*, 24–29.
24. Zeng, J.; Wu, Y.; Lin, Q. Researches on the compressive mechanics properties of steel fiber RPC. *J. Fuzhou Univ. Nat. Sci.* **2005**, *33*, 132–137.
25. Cao, X.; Peng, J.; LI, W. Study on mechanics properties of reactive powder concrete with different fibers.
Chin. Concr. Cem. Product. **2014**, *10*, 54–57.
26. Guo, T.; Teng, T.; Yu, Q. Influence of steel fibers contents on the strength and ductility of RPC. *City House* **2016**, *23*, 119–121.
27. Jia, F.; Wang, W.; He, K.; Xia, Y.; Wang, J.; Zha, Y.; Kong, D. Study on basic properties of reactive powder concrete with different fiber. *Chin. Concr. Cem. Product.* **2016**, *9*, 53–56.
28. Wang, Z.; Wang, J.; Yuan, J. Study on the Aggregates and mix Proportion of RPC. In Proceedings of the 13th National Academic Conference on Concrete and Prestressed Concrete, Beijing, China, 1 January 2016; pp. 342–347.
29. Al-Tikrite, A.; Hadi, M.N.S. Mechanical properties of reactive powder concrete containing industrial and waste steel fibers at different ratios under compression. *Construct. Build. Mater.* **2017**, *154*, 1024–1034. [CrossRef]
30. Maroliya, M.K. An investigation on reactive powder concrete containing steel fiber and fly ash. *Int. J. Eng.*
Technol. Adv. Eng. **2012**, *2*, 538–545.
31. Ministry of Housing and Urban-Rural Development of the People's Republic of China (MOHURD). *JGJ/T 221-2010: Technical Specification for Application of Fiber Reinforced Concrete*; China Ministry of Construction, China Architecture & Building Press: Beijing, China, 2002.
32. Swamy, R.N.; Mangat, P.S. A theory for the flexural strength of steel fiber reinforced concrete. *Cem. Concr. Res.* **1974**, *4*, 313–325. [CrossRef]
33. Choi, W.K. An experimental study on the flexural strength of fiber reinforced concrete structure. *Int. J. Saf.* **2012**, *11*, 26–28.
34. Nataraja, M.C.; Dhang, N.; Gupda, A.P. Stress-strain curves for steel fiber reinforced concrete under compression. *Cem. Concr. Compos.* **1999**, *21*, 383–390. [CrossRef]
35. Ezeldin, A.S.; Balaguru, P.N. Normal and high strength fiber reinforced concrete under compression. *J. Mater. Civil Eng.* **1992**, *4*, 415–429. [CrossRef]
36. Ou, Y.C.; Tsai, M.S.; Liu, K.; Chang, K.C. Compressive behavior of steel fiber-reinforced concrete with a high index. *J. Mater. Civil Eng.* **2012**, *24*, 207–215. [CrossRef]
37. Nehdi, M.L.; Soliman, A.M. Artificial intelligence model for early-age autogenous shrinkage of concrete.
ACI Mater. J. **2012**, *109*, 353–362.
38. Cascardi, A.; Micelli, F.; Aiello, M.A. An artificial neural networks model for the prediction of the compressive strength of FRP-confined concrete circular columns. *Eng. Struct.* **2017**, *140*, 199–208. [CrossRef]
39. Açikgenç, M.; Ulas¸, M.; Alyamaç, K.E. Using an Artificial Neural Network to Predict Mix Compositions of Steel Fiber-Reinforced Concrete. *Arab. J. Sci. Eng.* **2015**, *40*, 407–419. [CrossRef]

40. Vidivelli, B.; Jayaranjini, A. Prediction of compressive strength of high performance concrete containing industrial by products using artificial neural networks. *Int. J. Civil Eng. Technol.* **2016**, *7*, 302–314.
41. Altun, F.; Kis¸i, Ö.; Aydin, K. Predicting the compressive strength of steel fiber added lightweight concrete using neural network. *Comput. Mater. Sci.* **2008**, *42*, 259–265. [CrossRef]
42. Zealakshmi, D.; Ravichandran, A.; Kothandaraman, S. Prediction of Flexural Performance of Confined
Hybrid Fibre Reinforced High Strength Concrete Beam by Artificial Neural Networks. *Ind. J. Sci. Technol.* **2016**, *9*, 1–6. [CrossRef]
43. Sobhani, J.; Najimi, M.; Pourkhorshidi, A.; Parhizkar, T. Prediction of the compressive strength of no-slump concrete: A comparative study of regression, neural network and ANFIS models. *Construct. Build. Mater.* **2010**, *24*, 709–718. [CrossRef]
44. Golafshani, E.M.; Rahai, A.; Sebt, M.H.; Akbarpour, H. Prediction of bond strength of spliced steel bars in concrete using artificial neural network and fuzzy logic. *Construct. Build. Mater.* **2012**, *36*, 411–418. [CrossRef]
45. Sarıdemir, M. Predicting the compressive strength of mortars containing metakaolin by artificial neural networks and fuzzy logic. *Adv. Eng. Softw.* **2009**, *40*, 920–927. [CrossRef]
46. Alshihri, M.M.; Azmy, A.M.; El-Bisy, M.S. Neural networks for predicting compressive strength of structural light weight concrete. *Construct. Build. Mater.* **2009**, *23*, 2214–2219. [CrossRef]
47. China Standardization Administration. *GB/T 31387-2015: Code for Reactive Powder Concrete, China Standardization Administration*; China Architecture and Building Press: Beijing, China, 2015.
48. Mansur, M.; Islam, M. Interpretation of concrete strength for nonstandard specimens. *J. Mater. Civil Eng.* **2002**, *14*, 151–155. [CrossRef]
49. Lu, X.; Wang, Y.; Fu, C.; Zheng, W. Basic mechanical properties indexes of reactive powder concrete. *J. Harbin Inst. Techanol.* **2014**, *46*, 1–10.
50. Benjamin, G.; Marshall, D. Cylinder or sube: Strengtrhtesting of 80 to 200 MPa (11.6 to 29 ksi) ultra-high-performance fiber-reinforced concrete. *J. ACI Mater.* **2008**, *105*, 603–609.
51. Kusumawardaningsih, Y.; Fehling, E.; Ismail, M. UHPC compressive strength test specimens: Cylinder or cube. *Procedia Eng.* **2015**, *125*, 1076–1080. [CrossRef]